Journal of Environmental Management 271 (2020) 110884

Contents lists available at ScienceDirect

Journal of Environmental Management

journal homepage: http://www.elsevier.com/locate/jenvman

Research article

Valorization of bottom ash fines by surface functionalization to reduce leaching of harmful contaminants

Qadeer Alam, Thomas Dezaire, Florent Gauvin *, A.C.A. Delsing, H.J.H. Brouwers

Department of the Built Environment, Eindhoven University of Technology, P. O. Box 513, 5600, MB, Eindhoven, the Netherlands

ARTICLE INFO

Keywords:
Functionalization
Hydrophobicity
Surface characterization
MSWI bottom Ash
Leaching

ABSTRACT

This paper focuses on the functionalization of heterogeneous and highly contaminated waste material, namely bottom ashes (BA) with a particle size ≤ 125 μm that cannot be recycled with conventional treatments. The main goal of this study is to modify this waste into a valuable material that can be used in various applications, especially in the building sector. The complex mineralogical nature of this material was investigated with quantitative XRD, which confirms the presence of crystalline and amorphous phases such as silicates, carbonates, metallic oxides and amorphous glass. A hydrophobic modification was performed by using a fluorosilane grafting agent that utilizes the reactive surface sites of these minerals to form silanol bonds. Results showed that the 2.5% (m/m) of silane made the BA hydrophobic. Moreover, a thorough characterization showed that fluorosilane was well-grafted at the surface of the BA, with more than 60% of the fluorosilane chemisorbed on the surface. Additionally, the hydrophobic modification led to a significant decrease of the leaching of the contaminants (Cr, Cu, Mo and Sb) from the BA particles. Following this methodology, fine fraction of BA could be eventually used as a building material, preventing the landfill of this toxic waste.

1. Introduction

Over the past decades, hydrophobic materials have attracted great attention in academic and industrial fields because of the usefulness in both fundamental research and commercial applications (Ho Sun Lim et al., 2006). Indeed, hydrophobic materials have been used to fill and reinforce polymers, to improve various properties such as shrinkage, thermal expansion, creep as well as their mechanical behavior (Lotfipour et al., 2004; Murphy, 1966; Rong et al., 2006). Many different materials can be used as filler or reinforcing agents such as aerogels (Reynolds et al., 2001), zeolites (Sakthivel et al., 2013), calcite ($CaCO_3$) (Karakaş; Çelik, 2012), synthetic sorbents such as polypropylene (Li et al., 2014) and polyurethane (Li et al., 2012). However, the global filler market is already estimated as between 5 and 10 million tons per years and the growing use of synthetic particles encourages the development of hydrophobic materials, that are derived from economical and more sustainable raw materials (Pukánszky, 1999).

Industrial waste by-products such as incineration ashes (e.g., fly ashes) are often investigated as a replacement of the primary raw materials in polymer composites (Fakher et al., 2020; Labella et al., 2014). Another major incineration residue is bottom ash (BA), but as compared to fly ashes, these residues are highly heterogeneous because they are a mixture of different residual materials, such as ceramics, metals, organics, incineration slag and glass (Kirby and Rimstidt, 1993). As a waste material, BA is abundantly available and a preferred raw material considering the need to move to a circular economy (Lin et al., 2012; Toraldo et al., 2013). However, recycling this material remains a challenge because of the high leaching levels of contaminants (Luo et al., 2019; Saffarzadeh et al., 2015; Santos et al., 2013; Saqib and Bäckström, 2016; Yao et al., 2010) and stricter leaching limits imposed by EU and regional regulations (*Soil Quality Decree*, n.d.). The content of these contaminants strongly depends upon the particle size of the BA and the smaller particles are reported to be the most contaminated ones (Alam et al., 2016; Chimenos et al., 2003). Generally, size-separation of the BA particles is applied for recycling purposes (Alam et al., 2017; Tang et al., 2016). This process leads to the generation of fine particles, which are heavily contaminated and cannot be recycled with commonly applied treatment methodologies. These finer particles (≤125 μm) of BA can be recycled as a replacement of the primary fillers, such as calcite, silica, etc. However, like many other conventional fillers, BA is hydrophilic and would have very low compatibility with polymers, limiting its potential applications. Therefore, surface modification is required to functionalize

* Corresponding author.
E-mail address: f.gauvin@tue.nl (F. Gauvin).

https://doi.org/10.1016/j.jenvman.2020.110884
Received 30 March 2020; Received in revised form 27 May 2020; Accepted 29 May 2020

the BA by grafting a hydrophobic layer on its surface via a chemical reaction.

Currently, silane-coupling agents are the most commonly used for surface modification because they can easily react with oxides, forming strong and durable bonds. Moreover, a wide variety of silane is available, capable of imparting numerous surface properties depending on the organofunctional group of the silane (Kulinich and Farzaneh, 2004; Wang et al., 2010). Fluorosilanes have already been used to increase the hydrophobicity (Xu et al., 2012) of $CaCO_3$ nanoparticles and its interfacial compatibility with different matrices (Demjén et al., 1997; Yang et al., 2013). Numerous publications and patents have been dedicated to the utilization of silane on metallic oxides such as SiO_2 (Rowell, 2006; Yildirim et al., 2011), TiO_2 (Song et al., 2010), Al_2O_3 (Bao et al., 2013), titanate nanotubes (Chao et al., 2013) and even cellulosic materials such as cotton (Erasmus and Barkhuysen, 2009). Silane modification of BA can be challenging because of the high heterogeneity of this material in terms of chemical composition and morphology (Alam et al., 2019c; Schollbach et al., 2016). Nevertheless, a major portion of BA particles consists of calcite, metal-oxide, glass and silicates that could act as an active site, containing hydroxyl groups, which can react with silane allowing the modification (Alam et al., 2019a). Furthermore, silanes are expensive chemical reagent to use for the surface modifications; therefore, optimizing the amount of silane needed to achieve desired surface properties is of paramount importance.

As compared to most of the current research which focuses on modification of homogeneous materials (e.g. spherical silica) with well-known surface composition, this work aims to study the modification of heterogeneous materials such as BA fines (<0.125 mm). Indeed, this material has a non-conventional shape, heterogeneous functional group distribution at its surface and is contaminated by various elements such as Copper, Chromium or Vanadium, and could be used as state-of-the-art example in the field of material surface modification. Therefore, in this work, BA was modified by a fluorosilane coupling agent to introduce hydrophobic functionality into it. Hydrophobic functionalization of the <0.125 mm fraction with a silane coupling agent was investigated by developing a wet-chemistry method to graft 1H, 1H, 2H, 2H-perfluorooctyltriethoxysilane onto the BA surface. After functionalization, the hydrophobicity was assessed by measuring the water contact angle of the modified BA. Leaching tests to assess the mobility of heavy metals were performed with both original and hydrophobic BA to understand the influence of hydrophobic functionalization. The surface characterization after the silane modification was performed by XPS. Then, TGA was used to characterize and quantify the physisorbed and chemisorbed silane at the BA surface. GC-MS was performed on the TGA exhaust gas to confirm the previous observations made with other methods. Thanks to this in-depth analysis, a possible surface modification mechanism was proposed, showing which fraction of the BA can be modified and how it affects its hydrophobic properties.

2. Materials and methods

2.1. Materials

MSWI ≤4 mm was provided by Heros Sluiskil, the Netherlands. The BA fraction with a particle size of ≤0.125 mm was obtained by sieving using a vibratory sieve shaker (Retsch AS 450 Basic) according to DIN EN 933–1. Hereafter, this fraction of the BA will be referred to as BA-S. The silane form the modification was 1H, 1H, 2H, 2H-perfluorooctyltriethoxysilane (FS) with the purity of 98% and was obtained from Sigma-Aldrich. NaOH tablets (≥97.0%) and 32% HCl for pH alteration, and ultrapure HNO3 (58–60%) were obtained from VWR Chemicals. Dehydrated ethanol was purchased from Biosolve.

2.2. Hydrophobic functionalization

Hydrophobic BA was prepared by reflux, mixing 5 g of original BA-S and up to 7% (m/m) of FS for 5 h in a round bottom flask in a solution with 200 ml of ethanol/water (ratio 3:1). Before the BA-S was added, the functionalizing agent was activated by hydrolysis in the 200 ml of ethanol/water (ratio 3:1), under stirring for 1 h at 50 °C, with a pH of 3–4. The reaction temperature was controlled by heating the mixture in a water bath on a combined heating/stirring plate. After the functionalization, BA-S was separated from the reaction mixture using vacuum filtration and dried overnight at 60 °C to evaporate the residual solvent. Hereafter, this modified BA-S will be referred to as BA-S-F.

2.3. Material characterization

Bulk chemical composition of original BA-S was determined with an X-ray fluorescence spectrometer (XRF; PANalytical Epsilon 3, standardless) using fused beads. For XRF sample preparation, the loss on ignition (LOI) was measured at 1000 °C. The residues after LOI were homogenized with flux (Li_2BO_7 & $LiBO_4$) and non-wetting agent (LiBr) and a melt were prepared with fluxer oven (classisse leNeo) at 1100 °C. This melt was cast to prepare the fused bead sample for the analysis.

The X-ray diffraction (XRD) pattern was measured on a Bruker D2 (radiation source: Co $K\alpha_1$ 1.7901 Å, $K\alpha_2$ 1.7929, Detector: LynxEye, Divergence slit: fixed and soller slits: 2.5) to analyze the mineral composition. An internal standard (Si: 10% m/m) was added to the sample for the quantification of crystalline and amorphous phases. Phase identification and quantification were performed with the software X'Pert Highscore Plus (PANalytical) and TOPAS 4.2 (Bruker), respectively.

After functionalization, the hydrophobicity of functionalized BA-S was assessed with static water contact angle (CA) measurements using sessile drop technique (Dataphysics CA Systems OCA, TBU 90 E). The modified BA-S samples were prepared as a pressed powder tablet of 5 g by applying a pressure of 40 kN for 1 min in pellet press set. The volume of each water droplet was exactly 2.000 µl. Reported CA values correspond with the average measured CA of five water droplets on the pellet. The margin of error was defined as the 95% confidence interval of the standard deviation in these five measurements.

X-ray photoelectron spectroscopy (XPS) was performed by using a Thermo Scientific K-alpha spectrometer (source: monochromatic Al K_α x-rays) to analyze the elemental composition of BA before and after functionalization.

Thermogravimetric analysis (TGA; PerkinElmer Pyris 6 TGA 400 System) was performed on 10–15 mg of BA, in the temperature range 45–500 °C at a heating rate of 1 °C min^{-1}, under an N_2 flow of 40 ml min^{-1}. The exhaust gas flow from TGA was captured in 3 parallel connected gas sorption tubes in the temperature ranges 295–305 °C and 415–425 °C, and subsequently analyzed with combined gas chromatography (GC; PerkinElmer Clarus® 680) and mass spectrometry (MS; PerkinElmer Clarus® SQ 8 T) for qualitative analysis. These samples were introduced into the instrument via thermal desorption (PerkinElmer TurboMatrix 350).

2.4. Leaching analysis

The leaching potential of heavy metals, Cl^-, and SO_4^{2-} from original and modified BA-S was evaluated with a one-batch leaching test according to EN 12457–2 (Comite Europeen de Normalisation, 2002). The leachate samples from the test were acidified (pH 2) with 0.2 vol % ultrapure HNO_3 to avoid precipitation of metallic species. The leachates were analyzed for the trace elements with inductively coupled plasma-optical emission spectrometry (ICP-OES; Varian 730-ES). The contents of Cl^- and SO_4^{2-} were determined with ion-exchange chromatography (IC; Dionex 1100) equipped with an ion-exchange column AS9-HS (2 × 250 mm). For these measurements, a 9 mM solution of Na_2CO_3 was used as eluent with an isocratic flow of 0.25 ml min^{-1}, and the ions were detected by measuring the suppressed conductivity using an electrolytically regenerated suppressor (Dionex AERS 500, 2 mm).

3. Results and discussions

3.1. Characterization of BA

The chemical composition of the BA-S is provided in Table 1. It can be seen that this fraction of bottom ash is rich in CaO but also contains SiO_2, Al_2O_3 and Fe_2O_3 in decreasing order of abundance. Additionally, it also contains many trace elements such as Zn, Cu, Sb and Mn. The high content of CaO in this fraction is in accordance with the reported trend in which CaO content is inversely proportional to the particle size of bottom ash (Alam et al., 2019b, 2017; Yang et al., 2014).

Fig. 1 shows the diffraction pattern and mineral quantification of BA-S. The crystalline component of BA-S contains numerous mineral phases, most abundant one among them is calcite (calcium carbonate) and it is in accordance with the chemical composition. These crystalline phases can be grouped as follows: **1)** silicates with quartz, feldspar and melilite; **2)** iron (or metal) oxides with spinel, hematite, lepidocrocite and rutile, **3)** salts with halite, gypsum; **4)** the rest of crystalline phases with ettringite, apatite and zeolite. Moreover, the content of crystalline and amorphous phase in this fraction is 48 and 52% (m/m), respectively. The full profile Rietveld quantitative analysis performed with TOPAS software is provided in Appendix A (Fig. A1). The amorphous phase represents the sum of all amorphous phases in this fraction. These amorphous phases are reported to be incineration slag, bottle glass and other poorly crystalline phases (Alam et al., 2019b, 2019c). As expected, the bottom ashes are very heterogeneous and their functionalization can be challenging due to their complex mineralogical matrix. From the functionalization point of view, this material shows a diverse range of minerals that were formed under either incineration conditions or the weathering process after the incineration. The reported studies in the literature mostly concern the modification of pure phases such as glass, silica and carbonates with a well-defined composition and surface (Alam et al., 2019a; Araujo et al., 1995; Mihajlović et al., 2009).

The morphology and internal structure of BA-S particles are presented in Fig. 2a. These particles show random shape and sizes. The bright spots indicated the presence of metallic inclusions. In Fig. 2b the particle size distribution of BA-S is given and it can be seen that the d_{90} of this BA fraction is 88 μm. Although the particle size distribution of BA-S is similar to fly ash, their morphology is completely random and different as compared to the spherical particles of fly ashes. Due to the morphology of fly ash particles and relatively homogenous surface characteristics, they are widely used for hydrophobic functionalization. On the other hand, the complex mineral compositions, random particle shapes and heterogeneous surface characteristics of the BA hampers their functionalization. The FT-IR spectrum of the original bottom ash fraction shows characteristic bands (presented in Appendix A, Fig. A2) for water (1636 cm^{-1}), sulfate group (1414 cm^{-1}), Si–OH group (967 and 711 cm^{-1}) and carbonate group (872 cm^{-1}) (Liang et al., 2012; Reig et al., 2002).

3.2. Hydrophobicity assessment of modified BA-S

To characterize the effect of the fluorosilane modification on the hydrophobicity of the BA-S-F, contact angle measurements were performed by a sessile drop technique. Fig. 3 shows the average contact angle measured as a function of the weight fraction of silane used during the modification process, varying from 1 to 7% (m/m). The heterogeneity of the BA-S explained the larger standard deviation for some samples (e.g., at 1 and 5% m/m silane fraction).

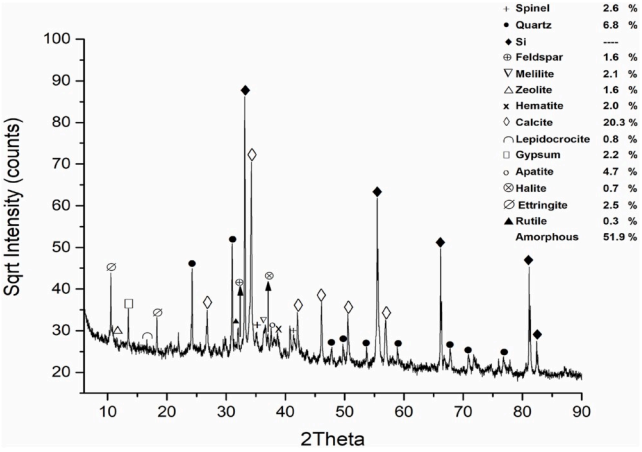

Fig. 1. X-ray diffraction pattern of BA-S along with the quantification of the mineral phases via Rietveld method.

BA-S is a hydrophilic material and as soon as the droplet of touches the tablet, it is absorbed immediately (Video S1, see SI). Results show that a small amount of silane (1% m/m) was able to increase the contact angle of the BA-S significantly, with values above 50°. Then, a linear increase of the contact angle was observed by addition of 1 and 2.5% (m/m) fluorosilane, showing that in this range, the BA-S still had available sites that could react with the functionalizing agent. Moreover, from 2% (m/m) of silane onwards, the contact angle was above 90°, which means that the sample can be considered hydrophobic (Video S2, see SI). From 2.5% (m/m) of silane, a plateau was reached, with contact angles above 130°, close to the superhydrophobic range (i.e., 145–150°). Above this value, the additional silane cannot react with the reactive sites of BA-S. In overall, the surface modification of BA-S by fluorosilane was a success and these results showed that the optimum weight fraction of silane that should be used was 2.5% (m/m). Yet, for the next tests in this study, a weight fraction of 5.1% (m/m) of silane was used because **1)** from these results, 2.5 or 5.1% (m/m) provide the same surface modification and **2)** 5% (m/m) allowed a better accuracy in all other the characterization measurements.

Supplementary video related to this article can be found at https://doi.org/10.1016/j.jenvman.2020.110884

3.3. Leaching analysis

The leaching potential of the original unmodified BA-S and functionalized materials are presented in Table 2. The original material contained numerous toxic elements that can be leach such as Cr, Cu, Mo, Sb, As, into the environment. The leaching potential of the functionalized BA-S is expected to decrease due to two factors as follows: 1) the functionalization protocol itself; 2) reduced compatibility between water and functionalized particles. The BA-S was modified in an ethanol/water mixture and under these conditions, mineral phases with limited stability dissolve and release the PTEs associated with them. For instance, ettringite can be dissolved under prolonged contact with water and is known to immobilize numerous PTEs, such as Sb, Cr, Cu and Zn (Alam et al., 2017) (Piantone et al., 2004). The other main factor leading to the decrease in the leaching of PTEs is the greater hydrophobicity of modified BA-S, which limits the wetting of these particles in the water, thereby reducing the leaching of contaminants. After modification, the

Table 1
Chemical composition of MSWI bottom ash (BA-S) with particle size ≤ 125 μm in % (m/m) measured with XRF. R.O: Remaining oxides and LOI: Loss on Ignition at 1000 °C.

	CaO	SiO_2	Al_2O_3	Fe_2O_3	SO_3	MgO	P_2O_5	TiO_2	ZnO	K_2O	Sb_2O_3	MnO	CuO	R.O.	LOI
BA-S	25.0	19.6	12.6	6.3	3.7	1.7	1.6	1.4	0.8	0.5	0.3	0.2	0.2	0.3	25.8

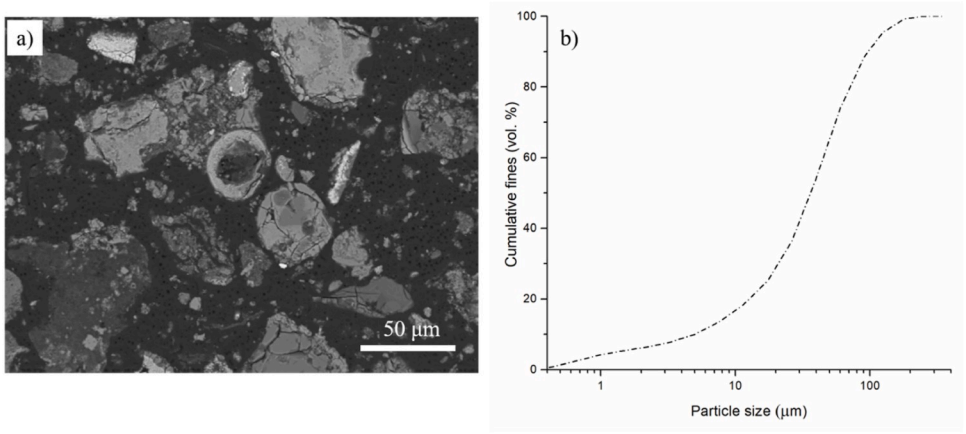

Fig. 2. a) SEM image of the cross-section of BA-S obtained in BSE (backscattered electron) mode and **b)** Particle size distribution of the BA-S fraction with particle size ≤ 125 μm.

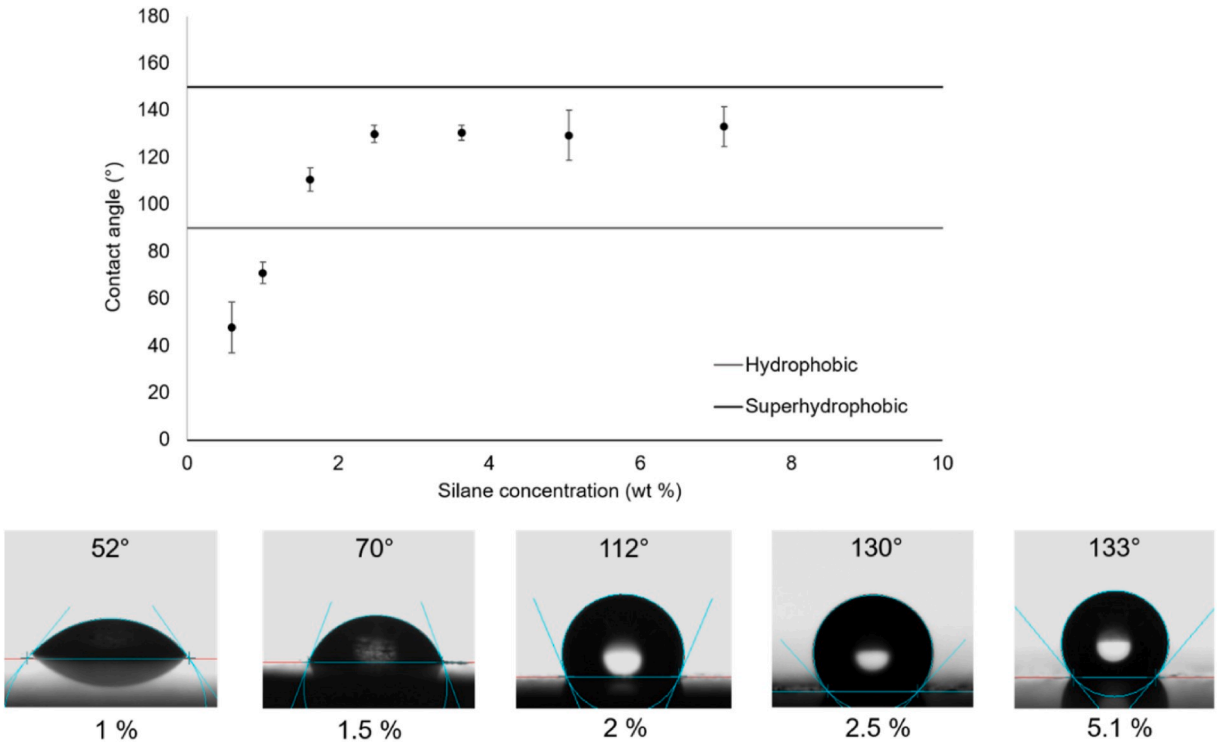

Fig. 3. Contact angle of the BA as a function of the silane weight fraction used during the modification process. Straight lines define the hydrophobic range (gray line, > 90°) and superhydrophobic range (black line, > 150°).

most significant decrease concerning leaching was noted in the case of Cu, with a decrease of more than 60% (m/m) as compared to original BA-S. Moreover, the leaching of Cr, Sb, and Cl^- and was also reduced significantly. On the other hand, an increase in the leaching of Zn and Ba was observed. Although an increase of the hydrophobicity was imparted to BA-S due to the functionalization, these results indicate that not all the mineral phases in the sample were modified, which is expected because of the complex mineral composition of the BA-S where not all the mineral phases present in BA-S have reactive sites that can interact with the FS functionalizing agent.

3.4. Silane – bottom ash interactions

X-ray photoelectron spectroscopy was performed to characterize the surface modification of the original and modified BA-S. Results are shown in Table 3. The XPS elemental analysis of the reference BA-S confirmed the results of previous sections, showing that it was composed of oxides (O = 63.6%) and more specifically calcium oxide (Ca = 9.6%) and aluminum oxide (Al = 7.4%). A significant amount of carbon was measured (C = 17.4%), which correspond to the organic compounds composing the BA-S.

After modification, more than 21% of fluorine was measured, corresponding to the silane, containing 13 fluorine per molecule, covering the surface of the BA. Moreover, a significant decrease in oxygen and calcium was observed, whereas the aluminum content was unchanged. This phenomenon shows that the fluorosilane mainly bonded to the calcium oxides present at the BA-S surface and not with aluminum species, showing the preferable interaction between the silane and the calcium oxides. This observation validates the mechanism proposed previously (see Section 3.2.). Moreover, it also indicates that the silane is

Table 2
A comparison between the leachable content of PTEs, chloride and sulfates from the original BA-S and BA-S-F with 5.1% (m/m) of the functionalizing agent, along with the leaching limits as per Soil Quality Decree (*Soil Quality Decree*, n. d.).

Elements/Ions	Leaching limits [mg/kg]	BA-S [mg/kg]	BA-S-F [mg/kg]
Ba	22	L.D.	0.47
Cr	0.63	1.20	0.87
Cu	0.90	6.61	2.59
Mo	1.00	1.12	0.98
Sb	0.32	0.97	0.76
As	0.90	0.16	0.17
Cd	0.04	L.D.	L.D.
Co	0.54	0.05	0.05
Pb	2.30	L.D.	0.03
Ni	0.44	0.07	0.06
Se	0.15	L.D.	L.D.
Sn	0.40	L.D.	L.D.
V	1.80	0.16	0.13
Zn	4.50	0.47	1.07
Cl^-	616	11,136	537
SO_4^{2-}	2430	20,097	19,483

L.D: lower than detection limit

Table 3
The atomic percentage of elements on the surfaces (obtained via XPS) of the reference (BA-S which underwent the same modification protocol in the absence of FS) and the BA-S-F (FS: 5.14% m/m) BA.

Sample	O_{1s} (%)	Ca_{2p} (%)	C_{1s} (%)	Al_{2s} (%)	Na_{1s} (%)	F_{1s} (%)
BA-S	63.6	9.6	17.4	7.4	1.9	–
BA-S-F	40.5	6.7	23.7	7.3	–	21.6
Pure fluorosilane[a]	12	–	32	–	–	52

[a] The theoretical weight percentage of elements in pure fluorosilane.

chemically bonded to the BA-S via silanol bonds and does not cover the other parts of the sample. Any physisorption would occur close to the calcium oxides and the chemisorbed silane itself, forming weak interactions with unreacted silane at the surface.

Further tests using the thermogravimetric analysis were performed to validate these observations. Fig. 4a shows the TGA curve of the reference (BA-S underwent the same modification protocol in the absence of FS) and BA-S-F (modified with 5.14% m/m of fluorosilane). The curve corresponding to the reference shows that even without surface modification, an important mass loss happened (- 10.0% m/m). This mass loss was linear between 0 and 500 °C and corresponds to the loss of the moisture, hydrated water and residual organic matter such as cellulose decomposes during this temperature range (Lin et al., 2010). The curve corresponding to BA-S-F shows logically a greater mass loss in total (−15.2% m/m) than the reference one. As compared to the reference sample, the mass loss of the BA-S-F seems to have multiple slopes, the most prominent one was at around 250 °C. To study this phenomenon, a corrected curve, subtracting the reference from the modified sample is presented in Fig. 4b.

This curve shows 2 different mass loss regions: The first one from 50 to 210 °C, with a mass loss of 2.0% (m/m) and the second one from 210 to 500 °C, with a mass loss of 3.2% (m/m). The total mass loss of 5.2% (m/m) was equal to the initial amount of silane used during the modification process (5.14% m/m). Therefore, the total mass loss corresponds to the fluorosilane at the BA surface and the two regimes can explain how the silane was bonded to the BA. In the literature, different studies showed that at the low-temperature range, functionalizing agents were only physisorbed at the surface because the energy required to break the weak interactions was small. On the other hand, a chemisorbed molecule requires much more energy to be debonded (i.e., enough energy to break the chemical bond between the functionalizing agent and the particle) (Yamazaki et al., 2016). The silanol bonds, which connect the fluorosilane to the BA, have been reported to break in the 150–200 to 450–500 °C range, which corresponds precisely to the second weight loss (Papirer, 2000). Therefore, after modification, 3% (m/m) of fluorosilane was attached to the BA surface via chemical bonds whereas 2% (m/m) of fluorosilane was physisorbed to the first silane layer. This result also validates the observation made in Section 3.2., where the contact angle was not increased further after adding 2.5% (m/m) of fluorosilane.

In order to confirm this result, gas chromatography coupled with mass spectrometry was performed on a sample of BA-S-F collected at 300 °C in the exhaust of the TG analyzer, which should correspond to fluorosilane chemisorbed to the BA. Fig. 5 shows the gas chromatogram of the sample and Table 4 sums up the fragmentation results.

The chromatogram shows the six main fragments that were characterized by mass spectrometry (Appendix A: Fig. A3 – Fig. A8). Mass spectrograms were analyzed with MassFrontier software to identify the nature of the exhaust gas at 300 °C. The main peaks of the different mass spectrograms were characterized as smaller fragments of the fluorosilane, as shown in Table 2. Moreover, the main peak of the fluorosilane (m/z = 426) is not visible, proving that the silane, at 300 °C, cannot be physisorbed and starts to be fragmented. Indeed, the pyrolysis of fluorocarbon compounds leads to numerous small fragments that have already been characterized in the literature for similar structure

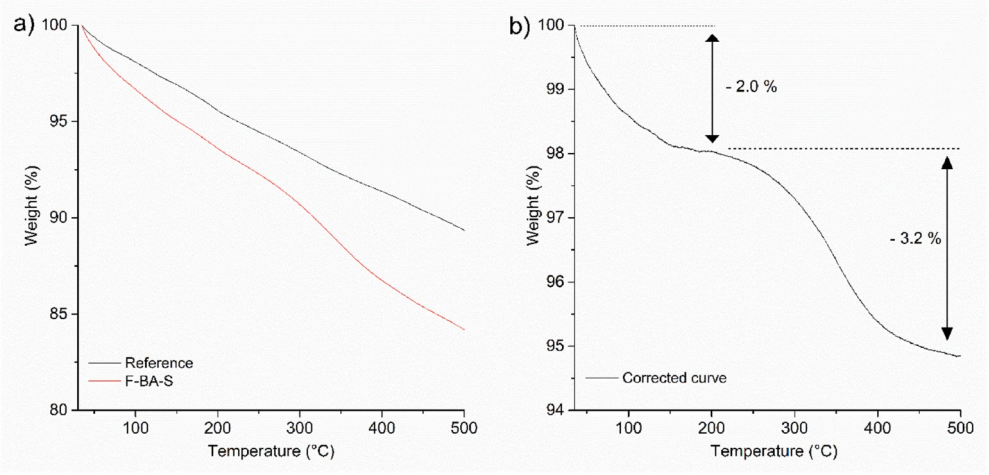

Fig. 4. Thermogravimetric analysis of **a)** BA-S functionalized with 5.14% (m/m) of FS, reference (BA-S underwent same modification protocol in the absence of FS) and **b)** corrected curve obtained by subtracting the mass loss due to the reference was from the mass loss of BA-S-F.

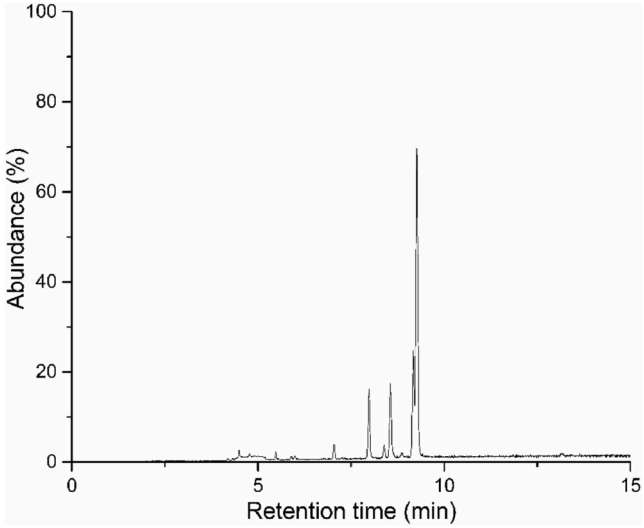

Fig. 5. Chromatogram of BA-S-F, corresponding to the TGA exhaust fumes sampled at 300 °C.

Table 4
Characterization of the fractionation of the Fluorosilane at 300 °C.

Chromatogram peaks (min)	m/z	Fluorosilane fragments
7.036	77	$SiO_2(OH)$
7.981	79	$Si(OH)_3$
8.386	109	$C_4H_4F_3$
8.556	119, 139, 308	C_2F_5, $C_5H_4F_4$, $C_6H_4F_8Si(OH)_3$
9.156	119, 139, 308	C_2F_5, $C_5H_4F_4$, $C_6H_4F_8Si(OH)_3$
9.276	59, 109	C_3H_4F, $C_4H_4F_3$

(Hiltz, 2014; Lonfei et al., 1986). Therefore, this characterization showed that the silane, above 300 °C, was well bonded to the BA-S and underwent a pyrolysis reaction.

4. Conclusions

The following conclusions are drawn from the present study:

- The fine fraction of bottom ash with particle size of ≤125 μm (BA-S) has been characterized to be heterogeneous, constituted of various crystalline phases which can be classified into silicates (quartz, feldspar and melilite), carbonates (calcite), metallic oxides (spinel, hematite and rutile), sulfate minerals (gypsum and ettringite) along with inorganic salts (halite). Moreover, the ration between crystalline and amorphous phases (mainly incineration slag and glass) was 48% and 52% (m/m), respectively.
- The minerals such as silicates, carbonates, metallic oxides and glass provide the reactive sites where silane modification can be performed to induce hydrophobic nature to the bottom ash particles.
- The silane modification of BA-S was successful. The hydrolyzed fluorosilane reacted primarily with calcium oxide at the surface of the BA. The hydrophobicity of the BA increases significantly; with contact angles up to 135°.
- The threshold of the weight fraction of fluorosilane that can react with the BA-S was characterized to be around 2.5–3% (m/m). Adding more fluorosilane did not increase the hydrophobicity of the BA-S because as characterized by TGA and GC-MS, the excess of silane cannot be chemically bonded to the active sites and but forms additional silane layers that are physisorbed to the BA.
- Moreover, leaching of potentially toxic elements Cr, Cu, Mo and Sb from the functionalized bottom ash was reduced by 28%, 61%, 13% and 22%, respectively. The decrease in the leaching is attributed to the functionalized protocol in which these contaminants were washed away and after the modification due to the hydrophobic nature of particles.

Declaration of competing interest

The authors declare that they have no known competing financial interests or personal relationships that could have appeared to influence the work reported in this paper.

Acknowledgments

The authors would like to acknowledge the financial support provided by NWO (Nederlandse Organisatie voor Wetenschappelijk Onderzoek), the Netherlands, under the project number 10019729: “Environmental concrete based on the treated MSWI bottom ashes”. Special thanks to Prof. dr. A. Caballero Martinez from the department of chemical engineering for assisting us with the XPS analysis.

Appendix A. Supplementary data

Supplementary data to this article can be found online at https://doi.org/10.1016/j.jenvman.2020.110884.

References

Alam, Q., Schollbach, K., Florea, M.V.A., Brouwers, H.J.H., 2016. Investigating washing treatment to minimize leaching of chlorides and heavy metals from MSWI bottom ash. In: 4th International Conference on Sustainable Solid Waste Management (Limassol, Cyprus).

Alam, Q., Florea, M.V.A., Schollbach, K., Brouwers, H.J.H., 2017. A two-stage treatment for Municipal Solid Waste Incineration (MSWI) bottom ash to remove agglomerated fine particles and leachable contaminants. Waste Manag. 67, 181–192. https://doi.org/10.1016/J.WASMAN.2017.05.029.

Alam, Q., Hendrix, Y., Thijs, L., Lazaro, A., Schollbach, K., Brouwers, H.J.H., 2019a. Novel low temperature synthesis of sodium silicate and ordered mesoporous silica from incineration bottom ash. J. Clean. Prod. 211, 874–883. https://doi.org/10.1016/j.jclepro.2018.11.173.

Alam, Q., Schollbach, K., Rijnders, M., van Hoek, C., van der Laan, S., Brouwers, H.J.H., 2019b. The immobilization of potentially toxic elements due to incineration and weathering of bottom ash fines. J. Hazard Mater. 379, 120798. https://doi.org/10.1016/J.JHAZMAT.2019.120798.

Alam, Q., Schollbach, K., van Hoek, C., van der Laan, S., de Wolf, T., Brouwers, H.J.H., 2019c. In-depth mineralogical quantification of MSWI bottom ash phases and their association with potentially toxic elements. Waste Manag. 87, 1–12. https://doi.org/10.1016/j.wasman.2019.01.031.

Araujo, Y.C., Toledo, P.G., Leon, V., Gonzalez, H.Y., 1995. Wettability of silane-treated glass slides as determined from X-ray photoelectron spectroscopy. J. Colloid Interface Sci. 176, 485–490. https://doi.org/10.1006/JCIS.1995.9942.

Bao, W., Guo, F., Zou, H., Gan, S., Xu, X., Zheng, K., 2013. Synthesis of hydrophobic alumina aerogel with surface modification from oil shale ash. Powder Technol. 249, 220–224. https://doi.org/10.1016/J.POWTEC.2013.08.001.

Chao, H.-P., Lee, C.-K., Juang, L.-C., Hsieh, T.-Y., 2013. Sorption of organic compounds with different water solubility on octadecyltrichlorosilane-modified titanate nanotubes. J. Taiwan Inst. Chem. Eng. 44, 111–116. https://doi.org/10.1016/J.JTICE.2012.08.005.

Chimenos, J.M., Fernández, A.I., Miralles, L., Segarra, M., Espiell, F., 2003. Short-term natural weathering of MSWI bottom ash as a function of particle size. Waste Manag. 23, 887–895. https://doi.org/10.1016/S0956-053X(03)00074-6.

Comite Europeen de Normalisation, 2002. EN 12457-2 Characterization of Waste - Leaching - Compliance Test for Leaching of Granular Waste Materials and Sludges - One Stage Batch Test at a Liquid to Solid Ratio of 10 L/kg for Materials with Particle Size below 4 Mm (Without or with Size Reduction.

Demjén, Z., Pukánszky, B., Földes, E., Nagy, J., 1997. Interaction of silane coupling agents with CaCO3. J. Colloid Interface Sci. 190, 427–436. https://doi.org/10.1006/JCIS.1997.4894.

Erasmus, E., Barkhuysen, F.A., 2009. Superhydrophobic cotton by fluorosilane modification. Indian J. Fibre Text. Res. 34, 377–379.

Fakher, S., Ahdaya, M., Imqam, A., 2020. Hydrolyzed polyacrylamide – fly ash reinforced polymer for chemical enhanced oil recovery: Part 1 – injectivity experiments. Fuel 260, 116310. https://doi.org/10.1016/j.fuel.2019.116310.

Hiltz, J.A., 2014. Characterization of fluoroelastomers by various analytical techniques including pyrolysis gas chromatography/mass spectrometry. J. Anal. Appl. Pyrolysis 109, 283–295. https://doi.org/10.1016/j.jaap.2013.06.008.

Karakaş, F., Çelik, M.S., 2012. Effect of quantity and size distribution of calcite filler on the quality of water borne paints. Prog. Org. Coating 74, 555–563. https://doi.org/10.1016/J.PORGCOAT.2012.02.002.

Kirby, C.S., Rimstidt, J.D., 1993. Mineralogy and surface properties of municipal solid waste ash. Environ. Sci. Technol. 27, 652–660. https://doi.org/10.1021/es00041a008.

Kulinich, S.A., Farzaneh, M., 2004. Hydrophobic properties of surfaces coated with fluoroalkylsiloxane and alkylsiloxane monolayers. Surf. Sci. 573, 379–390. https://doi.org/10.1016/j.susc.2004.10.008.

Labella, M., Zeltmann, S.E., Shunmugasamy, V.C., Gupta, N., Rohatgi, P.K., 2014. Mechanical and thermal properties of fly ash/vinyl ester syntactic foams. Fuel 121, 240–249. https://doi.org/10.1016/j.fuel.2013.12.038.

Li, H., Liu, L., Yang, F., 2012. Hydrophobic modification of polyurethane foam for oil spill cleanup. Mar. Pollut. Bull. 64, 1648–1653. https://doi.org/10.1016/J.MARPOLBUL.2012.05.039.

Li, H., Wu, W., Bubakir, M.M., Chen, H., Zhong, X., Liu, Z., Ding, Y., Yang, W., 2014. Polypropylene fibers fabricated via a needleless melt-electrospinning device for marine oil-spill cleanup. J. Appl. Polym. Sci. 131, n/a. https://doi.org/10.1002/app.40080.

Liang, Y., Ouyang, J., Wang, H., Wang, W., Chui, P., Sun, K., 2012. Synthesis and characterization of core–shell structured SiO2@YVO4:Yb3+,Er3+ microspheres. Appl. Surf. Sci. 258, 3689–3694. https://doi.org/10.1016/J.APSUSC.2011.12.006.

Lim, Ho Sun, Han, Joong Tark, Kwak, Donghoon, Meihua Jin, A., Cho, K., 2006. Photoreversibly Switchable Superhydrophobic Surface with Erasable and Rewritable Pattern. https://doi.org/10.1021/JA0655901.

Lin, Y.-C., Yen, J.-H., Lateef, S.K., Hong, P.-K.A., Lin, C.-F., 2010. Characteristics of residual organics in municipal solid waste incinerator bottom ash. J. Hazard Mater. 182, 337–345. https://doi.org/10.1016/j.jhazmat.2010.06.037.

Lin, C.L., Weng, M.C., Chang, C.H., 2012. Effect of incinerator bottom-ash composition on the mechanical behavior of backfill material. J. Environ. Manag. https://doi.org/10.1016/j.jenvman.2012.09.013.

Lonfei, J., Jingling, W., Shuman, X., 1986. Mechanisms of pyrolysis of fluoropolymers. J. Anal. Appl. Pyrolysis 10, 99–106. https://doi.org/10.1016/0165-2370(86)85009-4.

Lotfipour, F., Nokhodchi, A., Saeedi, M., Norouzi-Sani, S., Sharbafi, J., Siahi-Shadbad, M. R., 2004. The effect of hydrophilic and lipophilic polymers and fillers on the release rate of atenolol from HPMC matrices. Farmaco 59, 819–825. https://doi.org/10.1016/j.farmac.2004.06.006.

Luo, H., Cheng, Y., He, D., Yang, E.H., 2019. Review of leaching behavior of municipal solid waste incineration (MSWI) ash. Sci. Total Environ. https://doi.org/10.1016/j.scitotenv.2019.03.004.

Mihajlović, S., Sekulić, Ž., Daković, A., Vučinić, D., Jovanović, V., Stojanović, J., 2009. Surface properties of natural calcite filler treated with stearic acid. Ceram. - Silikaty 53, 268–275.

Murphy, T.P., 1966. Reinforced and filled thermoplastics. Ind. Eng. Chem. 58, 41–49.

Papirer, E., 2000. Adsorption on Silica Surfaces. CRC Press.

Piantone, P., Bodénan, F., Chatelet-Snidaro, L., 2004. Mineralogical study of secondary mineral phases from weathered MSWI bottom ash: implications for the modelling and trapping of heavy metals. Appl. Geochem. 19, 1891–1904. https://doi.org/10.1016/j.apgeochem.2004.05.006.

Pukánszky, B., 1999. Particulate Filled Polypropylene Composites. Springer, Dordrecht, pp. 574–580. https://doi.org/10.1007/978-94-011-4421-6_78.

Reig, F.B., Adelantado, J.V.G., Moya Moreno, M.C., 2002. FTIR quantitative analysis of calcium carbonate (calcite) and silica (quartz) mixtures using the constant ratio method. Application to geological samples. Talanta 58, 811–821. https://doi.org/10.1016/S0039-9140(02)00372-7.

Reynolds, J.G., Coronado, P.R., Hrubesh, L.W., 2001. Hydrophobic aerogels for oil-spill clean up – synthesis and characterization. J. Non-Cryst. Solids 292, 127–137. https://doi.org/10.1016/S0022-3093(01)00882-1.

Rong, M.Z., Zhang, M.Q., Ruan, W.H., 2006. Surface modification of nanoscale fillers for improving properties of polymer nanocomposites: a review. Mater. Sci. Technol. 22, 787–796. https://doi.org/10.1179/174328406X101247.

Rowell, F., 2006. Hydrophobic Silica Particles and Methods of Making Same. US 2007/0196656A1.

Saffarzadeh, A., Arumugam, N., Shimaoka, T., 2015. Aluminum and aluminum alloys in municipal solid waste incineration (MSWI) bottom ash: a potential source for the production of hydrogen gas. Int. J. Hydrogen Energy 41, 820–831. https://doi.org/10.1016/j.ijhydene.2015.11.059.

Sakthivel, T., Reid, D.L., Goldstein, I., Hench, L., Seal, S., 2013. Hydrophobic high surface area zeolites derived from fly ash for oil spill remediation. Environ. Sci. Technol. 47, 5843–5850. https://doi.org/10.1021/es3048174.

Santos, R.M., Mertens, G., Salman, M., Cizer, Ö., Van Gerven, T., 2013. Comparative study of ageing, heat treatment and accelerated carbonation for stabilization of municipal solid waste incineration bottom ash in view of reducing regulated heavy metal/metalloid leaching. J. Environ. Manag. https://doi.org/10.1016/j.jenvman.2013.06.033.

Saqib, N., Bäckström, M., 2016. Chemical association and mobility of trace elements in 13 different fuel incineration bottom ashes. Fuel 172, 105–117. https://doi.org/10.1016/j.fuel.2016.01.010.

Schollbach, K., Alam, Q., Caprai, V., Florea, M.V.A., Van der Laan, S.R., van Hoek, C.J.G., Brouwers, H.J.H., 2016. Combined chracterization of the MSWI bottom ash. In: Proceedings of the Thirty-Eighth International Conference on Cement Microscopy. Lyon, France, pp. 74–84.

Soil Quality Decree, n.d. , Ministerie van Volkshuisvesting, Ruimtelijke Ordeling en Milieubeheer. Regeling Bodemkwaliteit, VROM, Den Haag: ruimte en Milieu. Ministerie van Volkshuisvesting, (Ruimtelijke Ordeling en Milieubeheer).

Song, Y.Y., Hildebrand, H., Schmuki, P., 2010. Optimized monolayer grafting of 3-aminopropyltriethoxysilane onto amorphous, anatase and rutile TiO2. Surf. Sci. 604, 346–353. https://doi.org/10.1016/j.susc.2009.11.027.

Tang, P., Florea, M.V.A., Spiesz, P., Brouwers, H.J.H., 2016. Application of thermally activated municipal solid waste incineration (MSWI) bottom ash fines as binder substitute. Cement Concr. Compos. 70, 194–205. https://doi.org/10.1016/j.cemconcomp.2016.03.015.

Toraldo, E., Saponaro, S., Careghini, A., Mariani, E., 2013. Use of stabilized bottom ash for bound layers of road pavements. J. Environ. Manag. https://doi.org/10.1016/j.jenvman.2013.02.037.

Wang, C., Piao, C., Zhai, X., Hickman, F.N., Li, J., 2010. Synthesis and character of superhydrophobic CaCO3 powder in situ. Powder Technol. https://doi.org/10.1016/j.powtec.2010.02.016.

Xu, L., Karunakaran, R.G., Guo, J., Yang, S., 2012. Transparent, superhydrophobic surfaces from one-step spin coating of hydrophobic nanoparticles. ACS Appl. Mater. Interfaces 4, 1118–1125. https://doi.org/10.1021/am201750h.

Yamazaki, R., Karyu, N., Noda, M., Fujii, S., Nakamura, Y., 2016. Quantitative measurement of physisorbed silane on a silica particle surface treated with silane coupling agents by thermogravimetric analysis. J. Appl. Polym. Sci. 133, n/a. https://doi.org/10.1002/app.43256.

Yang, Z., Tang, Y., Zhang, J., 2013. Surface modification of caco3 nanoparticle with silane coupling agent for improvement of interfacial compatibility with sbr latex.pdf. Chalcogenide Lett. 10, 131–141.

Yang, S., Saffarzadeh, A., Shimaoka, T., Kawano, T., 2014. Existence of Cl in municipal solid waste incineration bottom ash and dechlorination effect of thermal treatment. J. Hazard Mater. 267, 214–220. https://doi.org/10.1016/j.jhazmat.2013.12.045.

Yao, J., Li, W.-B., Kong, Q.-N., Wu, Y.-Y., He, R., Shen, D.-S., 2010. Content, mobility and transfer behavior of heavy metals in MSWI bottom ash in Zhejiang province, China. Fuel 89, 616–622. https://doi.org/10.1016/j.fuel.2009.06.016.

Yildirim, A., Budunoglu, H., Daglar, B., Deniz, H., Bayindir, M., 2011. One-pot preparation of fluorinated mesoporous silica nanoparticles for liquid marble formation and superhydrophobic surfaces. ACS Appl. Mater. Interfaces 3, 1804–1808. https://doi.org/10.1021/am200359e.